Localization of Electro-elastic Shear Waves in a Periodically Stratified Piezoelectric Structure

D. Piliposyan[a], K. Ghazaryan[a], G. Piliposian[b,*]

[a] *Institute of Mechanics, 24 Bagramyan ave.,0019 Yerevan, Armenia*
[b] *Department of Mathematical Sciences, University of Liverpool, L69 7ZL, Liverpool, UK*

Abstract

We investigate the localization of electro-elastic shear waves traveling along a homogeneous piezoelectric supperlattice waveguide with thin electrodes periodically inserted parallel to the waveguide faces. The transfer matrix between two neighbouring sublayers is constructed based on the electrically shorted conditions on the electrodes. A relationship is established between elastic displacements of the top and bottom faces of the superlattice when these faces are traction free. When they are clamped a relationship is established between tangential stresses on the two faces. It is shown that due to the electro-mechanical coupling, waves can be localized at interfaces in the structure if the electrodes are non-uniformly distributed along the thickness of the piezoelectric waveguide. The localization of waves significantly increases with the number of non-symmetrically introduced electrodes between the layers. The results of the paper can be helpful in the design of narrow band filters or multi-channel piezoelectric filters.

Keywords: `piezoelectric, periodic, wave localization, transfer matrix`

---

1. Introduction

The problem of elastic wave propagation in piezoelectric structures is important due to extensive applications of piezoelectric materials in smart materials and structures. Often these structures are made of two or more different constituents arranged

*Corresponding author
Email addresses: `piliposyan@mechins.sci.am` (D. Piliposyan), `kghazaryan@mechins.sci.am` (K. Ghazaryan), `gayane@liverpool.ac.uk` (G. Piliposian)

periodically. These include thin film piezoelectric layered structures widely used in high frequency and performance, low cost, low energy consumption and small size technologies.

Electro-mechanical coupling in these structures strongly affects the properties of acoustic waves and leads to new and interesting properties [1, 2, 3, 4, 5]. Piezoelectric infinite periodic structures often referred to as phononic crystals are especially sensitive to the electric properties of the interfaces [6, 7, 8, 9]. Of particular interest are the properties of Bloch waves in piezoelectric phononic crystals. Investigation of frequencies of band gaps, standing waves, trapped and slow waves in periodic piezoelectric structures can lead to new developments in imaging devices and filtering of unwanted vibrations. Piezoelectric periodic waveguides with full contact interfacial conditions have been studied extensively [10],[11]. Electrically shorted interfaces represent a separate problem since they cannot be derived as a particular case from the solutions of full contact interfacial conditions. In this problems the solutions at interfaces become connected by degenerate matrices which cannot be inverted. For these problems the wave properties are represented by only one dispersion equation as opposed to two for full contact interfaces [12], [5].

Of special interest is the localization of waves in periodic structures which leads to a spatial decay of the wave amplitudes [13]. Localized modes in layered structures may have either positive or damaging effects. Wave and vibration localization makes it possible to control the propagation of waves and vibrations, leading to many new applications. On the other hand, localization can result in local energy concentrations which can affect the reliability and durability of engineering applications. In both cases, since small irregularities can lead to substantial consequences, it is crucial to investigate the underlying physical mechanisms of mode localization. Using local resonance theory, a shear wave attenuation in a thin beam with periodically attached local resonators has been investigated in [14]. The problem of flexural wave localization in a disordered periodic piezoelectric beam and the effects of several disorder parameters on the localization factor is studied in [15, 16, 17].

Leakage of vibrational energy in piezoelectric devices can cause fluctuations and degradation of the structure. If this energy is confined in a localized region of a periodic structure it would be possible to support the structure at non-vibrating areas and thus to design low loss and high reliability piezoelectric devices. Energy trapping of elastic waves and its application to piezoelectric devices including thickness vibrational energy trapped near electroded areas of a piezoelectric plate is investigated in [18]. The investigation of wave propagation in periodic piezoelectric structures have mostly been carried out for infinite periodicity micro-structures where the Bloch theorem can be applied to reduce the solution to the problem for a single unit cell. Understanding acoustic properties of wave propagation in finite periodic media is also vital since the number of periodic cells is finite in most realistic situations. Wave transmission properties of periodic microstructures of finite length and the influence of the finite-length periodicity on the wave transmission characteristics is discussed in [19].

Due to magneto-elastic coupling the periodic modulation of the electro-elastic properties of materials in the piezoelectric periodic structures made of two or more different constituents leads to new and exciting features in infinite and finite piezoelectric periodic structures. The same can also be expected in homogeneous or non homogeneous piezoelectric structures with periodically arranged metasurfaces, inclusions or cracks. The present paper investigates the oscillatory response of the shear wave transmission in a piezoelectric waveguide with thin electrodes arranged in a periodic way parallel to the waveguide top and bottom faces. A transfer matrix approach is adopted to investigate wave and vibration localization.

2. Statement of the Problem and Solution

We consider vibrations of a piezoelectric structure made of a finite stack of periodically stratified transversely isotropic hexagonal piezoelectric crystal structure (6mm) with the crystallographic axes directed along the Oz direction and accupying the region $0 < x < L$, $-\infty < y < \infty$ and $-\infty < z < \infty$ (Fig.1). The periodic structure consists of a stack of n cells each containing a pair of layers $(s = 1,2)$ made of the same piezoelectric material with thicknesses d_1 and d_2 $(d = d_1 + d_2)$ and separated by electrodes of negligible thickness (Fig.1). For an anti-plane problem $(\partial/\partial z = 0)$ in quasi-static approximation the interconnected electro-elastic excitations in a transversely isotropic

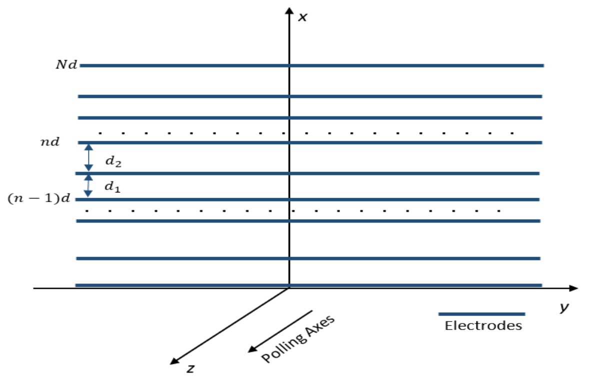

Figure 1: Piezoelectric superlattice made of finite number of cells.

hexagonal piezoelectric crystal are with respect to u_z, E_x and E_y [5]

$$\operatorname{div}\boldsymbol{\sigma} = \rho\frac{\partial\,\mathbf{u}}{\partial t}, \quad \operatorname{div}\boldsymbol{D} = 0, \quad \operatorname{curl}\mathbf{E} = \mathbf{0}, \quad \mathbf{E} = -\nabla\,\varphi, \tag{1}$$

$$\boldsymbol{\sigma} = \operatorname{div}(Gu + e_{15}\varphi), \quad \mathbf{D} = \nabla(-\varepsilon\varphi + e_{15}u), \tag{2}$$

$$\boldsymbol{\sigma} = (\sigma_{xz},\, \sigma_{yz}), \quad \mathbf{D} = (D_x, D_y), \quad \mathbf{E} = (E_x, E_y). \tag{3}$$

where σ_{xz} and σ_{yz} are shear stresses, $\mathbf{D}$, $\mathbf{E}$ and $\mathbf{u} = (0,0,u(x,y,t))$ are electric displacement, electric field, φ is the electric field potential, and the displacement vectors, ε, e_{15}, ρ and G are the dielectric permittivity, piezoelectric constant, mass density and shear modulus respectively, $\nabla = (\partial/\partial x, \partial/\partial y, 0)$.

Substituting the first relation in (2) into the first equation in (1) and taking into account the second relation in (2) and the second equation in (1) the anti-plane problem reduces to the system of the following equations:

$$c^2\Delta u - \frac{\partial^2 u}{\partial t^2} = 0, \quad \Delta\left(\frac{e_{15}}{\varepsilon}u - \varphi\right) = 0, \tag{4}$$

where $c = \sqrt{G_0/\rho}$ is the velocity of the shear wave in the medium, $G_0 = G(1+\chi)$, $\chi = \dfrac{e_{15}^2}{G\varepsilon}$ and $\Delta \equiv \dfrac{\partial^2}{\partial x^2} + \dfrac{\partial^2}{\partial y^2}$.

Consider partial transmission conditions of electrically shorted and elastically perfect contacts at the interfaces: $x_{n-1} = (n-1)d$, $\tilde{x} = nd + d_1$, and $x_n = nd$, $(n = 1, \ldots, N)$

$$\varphi(x_{n-1}, y, t) = 0, \quad \varphi(\tilde{x}, y, t) = 0, \quad \varphi(x_n, y, t) = 0, \tag{5}$$

$$[\sigma(x_{n-1}, y, t)] = 0,\ [u(x_{n-1}, y, t)] = 0,\ [\sigma(\tilde{x}, y, t)] = 0,\ [u(\tilde{x}, y, t)] = 0, \tag{6}$$

$$[\sigma(x_n, y, t)] = 0, [u(x_n, y, t)] = 0, \tag{7}$$

where $\sigma_0(x, y, t) = \sigma_{0xz}(x, y, z)$ and $[\cdot]$ is a jump of a function across the interfaces.

The solution of (4) for the displacement and the electric field potential can be written in the form of plane harmonic wave propagating along the y axis [20]:

$$u_s(x, y, t) = u_{0s}(x)\mathrm{e}^{\mathrm{i}(ky-\omega t)},\ \ \varphi_s(x, y, t) = \varphi_{0s}(x)\mathrm{e}^{\mathrm{i}(ky-\omega t)}, \tag{8}$$

where k and ω are real wave number and angular frequency. The solutions for $u_{0s}(x)$ and $\varphi_{0s}(x)$ are

$$u_{0s}(x) = C_{1s}\sin(qx) + C_{2s}\cos(qx), \tag{9}$$

$$\varphi_{0s}(x) = C_{3s}\sinh(kx) + C_{4s}\cosh(kx) + \frac{\varepsilon}{e}\left(C_{1s}\sin(qx) + C_{2s}\cos(qx)\right), \tag{10}$$

and the corresponding expression for the tangential stresses

$$\sigma_{0s}(x) = qG_0\left(C_{1s}\cos(qx) - C_{2s}\sin(qx)\right) + ke\left(C_{3s}\cosh(kx) + C_{4s}\sinh(kx)\right), \tag{11}$$

where $e = e_{15}$, $s = 1$ corresponds to the solutions for $x \in (x_{n-1}, \tilde{x})$ and $s = 2$ for $x \in (\tilde{x}, x_n)$, $C_{1s}, C_{2s}, C_{3s}, C_{4s}$ are arbitrary constants and $q = d^{-1}\sqrt{\vartheta^2 - (kd)^2}$, where $\vartheta = (\omega d)/c$ is the dimensionless frequency of electro-elastic vibrations.

It follows from (9) and (10) that in a one dimensional setting ($k = 0$) the solution corresponds to the solutions of the homogeneous waveguide with the piezoelectric effect present only in the elastic modulus.

Applying the boundary conditions (5) for $\varphi_0(x)$ at two consecutive interfaces the coefficients C_{3s} and C_{4s} can be expressed via C_{1s} and C_{2s} as follows

$$\begin{aligned} C_{3s} = \frac{e}{\varepsilon}\cosh\left(k(x_1 - x_2)\right)\left(C_{2s}\left(\cos(qx_{2s})\cosh(kx_{1s}) - \cos(qx_{1s})\cosh(kx_{2s})\right) + \right. \\ \left. + C_{1s}\left(\cosh(kx_{1s})\sin(qx_{2s}) - \cosh(kx_{2s})\sin(qx_{1s})\right)\right), \end{aligned} \tag{12}$$

$$C_{4s} = \frac{e}{\varepsilon}\cosh\left(k(x_1 - x_2)\right)\left(C_{2s}\left(\cos(qx_{1s})\sinh(kx_{2s}) - \cos(qx_{2s})\sinh(kx_{1s})\right) + \right.$$
$$\left. + C_{1s}\left(\sin(qx_{1s})\sinh(kx_{2s}) - \sin(qx_{2s})\sinh(kx_{1s})\right)\right). \quad (13)$$

Then from equation (9) and (11) the functions u_{0s} and σ_{0s} can br expressed via arbitrary constants C_{1s} and C_{2s} in the following matrix form

$$\mathbf{U}_s(x) = \mathbf{P}(x)\mathbf{C}_{0s}, \quad (14)$$

where

$$\mathbf{U}_s(x) = \begin{pmatrix} u_{0s}(x) \\ \sigma_{0xz}(x) \end{pmatrix},\ \mathbf{P} = \begin{pmatrix} \alpha & \beta \\ \gamma & \xi \end{pmatrix},\ \mathbf{C}_{0s} = \begin{pmatrix} C_{1s} \\ C_{2s} \end{pmatrix}, \quad (15)$$

and

$$\alpha = \sin(qx), \quad \beta = \cos(qx), \quad (16)$$

$$\gamma = G_0 q\cos(qx) + Q\ \left(\cosh(kx)\left(\cosh(kx_1)\sin(qx_2) - \cosh(kx_2)\sin(qx_1)\right)\ - \right.$$
$$\left. - \sinh(kx)\left(\sinh(kx_1)\sin(qx_2) + \sinh(kx_2)\sin(qx_1)\right)\right), \quad (17)$$

$$\xi = -G_0 q\sin(qx) + Q\ \left(\cosh(kx)\left(\cosh(kx_1)\cos(qx_2) - \cosh(kx_2)\cos(qx_1)\right)\ + \right.$$
$$\left. + \sinh(kx)\left(-\sinh(kx_1)\cos(qx_2) + \sinh(kx_2)\cos(qx_1)\right)\right), \quad (18)$$

$$Q = \frac{e^2 k}{\varepsilon}\csc(k(x_1 - x_2)). \quad (19)$$

In (19) $x_1 = x_{n-1}$, $x_2 = \tilde{x}$ for $s = 1$ and $x_1 = \tilde{x}$, $x_2 = x_n$ for $s = 2$. It follows from (14) that

$$\mathbf{U}_1(x_{n-1}) = \mathbf{P}(x_{n-1})\mathbf{C}_{01}, \quad \mathbf{U}_1(\tilde{x}) = \mathbf{P}(\tilde{x})\mathbf{C}_{01}, \quad (20)$$

$$\mathbf{U}_2(\tilde{x}) = \mathbf{P}(\tilde{x})\mathbf{C}_{02}, \quad \mathbf{U}_2(x_n) = \mathbf{P}(x_n)\mathbf{C}_{02}. \quad (21)$$

From the first equations (20) and (21) the unknown constants $\mathbf{C}_{01}$ and $\mathbf{C}_{02}$ are

$$\mathbf{C}_{01} = \mathbf{P}^{-1}(x_{n-1})\mathbf{U}_1(x_{n-1}), \quad \mathbf{C}_{02} = \mathbf{P}^{-2}(\tilde{x})\mathbf{U}_2(\tilde{x}). \quad (22)$$

Substitution (22) into the second equations of (20) and of (21) will eliminate the constants $\mathbf{C}_{01}$ and $\mathbf{C}_{02}$ giving

$$\mathbf{U}_1(\tilde{x}) = \mathbf{T}_1\mathbf{U}_1(x_{n-1}), \quad \mathbf{U}_2(x_n) = \mathbf{T}_2\mathbf{U}_2(\tilde{x}), \quad (23)$$

where $\mathbf{T}_1 = \mathbf{P}(\tilde{x})\mathbf{P}^{-1}(x_{n-1})$ and $\mathbf{T}_2 = \mathbf{P}(x_n)\mathbf{P}^{-1}(\tilde{x})$ are unimodal transfer matrices in each sub-domain

$$\mathbf{T}_s = \begin{pmatrix} t_{11} & t_{12} \\ t_{21} & t_{22} \end{pmatrix}, \tag{24}$$

with

$$t_{11} = t_{22} = \frac{q\cos(d_s q) - k\chi\coth(d_s k)\sin(d_s q)}{q - k\chi\operatorname{csch}(d_s k)\sin(d_s q)},$$

$$t_{12} = \frac{1}{\mathrm{G}_0(q\csc(d_s q) - k\chi\operatorname{csch}(d_s k))},$$

$$t_{21} = \frac{-\mathrm{G}_0(\sin(d_s q)\left((k\chi)^2 - q^2\right)) + 2kq\chi(\coth(d_s k)\cos(d_s q)) - \operatorname{csch}(d_s k))}{k\chi\operatorname{csch}(d_s k)\sin(d_s q) - q}.$$

Using the continuity condition of the displacement at the interfaces $\mathbf{U}_1(\tilde{x}) = \mathbf{U}_2(\tilde{x})$ and relation (22) the propagator matrix can now be constructed as

$$\mathbf{U}_2(x_n) = \mathbf{M}\mathbf{U}_1(x_{n-1}), \tag{25}$$

where $$\mathbf{M} = \mathbf{T}_2\mathbf{T}_1, \quad \mathbf{M} = \begin{pmatrix} m_{11} & m_{12} \\ m_{21} & m_{22} \end{pmatrix},$$

and

$$m_{11}(\vartheta) = \frac{\sin(d_1 q)\left(\sin(d_2 q)\left(k^2\chi^2 - q^2\right) - 2kqS_2\chi\right) + F_1F_2}{A_1A_2},$$

$$m_{12}(\vartheta) = \frac{F_1\sin(d_2 q) + F_2\sin(d_1 q)}{A_1A_2G_0},$$

$$m_{21}(\vartheta) = -\frac{G_0\left(\left(q^2 - k^2\chi^2\right)(F_1\sin(d_2 q) + F_2\sin(d_1 q)) + 2kq\chi(F_2S_1 + F_1S_2)\right)}{A_1A_2},$$

$$m_{22}(\vartheta) = \frac{\sin(d_2 q)\left(\sin(d_1 q)\left(k^2\chi^2 - q^2\right) - 2kqS_1\chi\right) + F_1F_2}{A_1A_2},$$

$$F_s = q\cos(qd_s) - k\chi\coth(kd_s)\sin(qd_s),$$

$$A_s = q - k\chi\operatorname{csch}(kd_s)\sin(qd_s),$$

$$S_s = \coth(kd_s)\cos(qd_s) - \operatorname{csch}(kd_s), \; s = 1, 2.$$

The matrix of the shear wave field connecting vector fields at the interface of the nth cell is unimodular [21]. This can be used to write the relationship between the field vectors at $x = 0$ and $x = Nd = L$

$$\mathbf{U}(L) = \mathbf{M}^N\mathbf{U}(0), \tag{26}$$

where following Sylvester's theorem [22] the elements for the matrix $\mathbf{M}^n$ can be written as follows

$$M_{11} = m_{11}(\vartheta)S_{n-1}(\eta) - S_{n-2}(\eta), \quad M_{12} = m_{12}(\vartheta)S_{n-1}(\eta),$$

$$M_{21} = m_{21}(\vartheta)S_{n-1}(\eta), \quad M_{22} = m_{22}(\vartheta)S_{n-1}(\eta) - S_{n-2}(\eta),$$

where $S_n(\eta)$ are the Chebyshev polynomials of second kind

$$S_n(\eta) = \frac{\sin((n+1)\phi)}{\sin(\phi)}, \quad \cos(\phi) = \eta, \quad \eta = \frac{1}{2}\mathrm{Tr}(\mathbf{M}) = \frac{1}{2}(m_{11}(\vartheta) + m_{22}(\vartheta)),$$

which can be calculated using the recurrence relation [22]

$$S_n(\eta) = 2\eta S_{n-1}(\eta) - S_{n-2}(\eta), \; n = 0, 1, 2, ... \tag{27}$$

2.1. Localisation Modes of a Traction Free Waveguide

Consider now a boundary value problem for traction free top and bottom faces. In this case the following matrix equation can be imposed:

$$\begin{pmatrix} M_{11} & M_{12} \\ M_{21} & M_{22} \end{pmatrix} \begin{pmatrix} u(0) \\ 0 \end{pmatrix} = \begin{pmatrix} u(L) \\ 0 \end{pmatrix}. \tag{28}$$

Equation (28) is equivalent to the following two equations

$$(m_{11}(\vartheta)S_{N-1}(\eta) - S_{N-2}(\eta))u(0) = u(L), \tag{29}$$

$$m_{21}(\vartheta)S_{N-1}(\eta)u(0) = 0. \tag{30}$$

It follows also from (26) that relations between $x = 0$ and $x = nd$ for any $n = 1, 2, ..., N$ can be written as

$$\begin{pmatrix} M_{11} & M_{12} \\ M_{21} & M_{22} \end{pmatrix} \begin{pmatrix} u(0) \\ 0 \end{pmatrix} - \begin{pmatrix} u(nd) \\ \sigma_0(nd) \end{pmatrix} = 0, \quad u(nd) = (m_{11}(\vartheta)S_{n-1} - S_{n-2})u(0). \tag{31}$$

Equation (30) gives two dispersion equations $m_{21}(\vartheta) = 0$ and $S_{N-1}(\eta) = 0$ which describe curves in the phase-plane (ϑ, kd), each point of which corresponds a propagating wave in the structure.

If $m_{21}(\vartheta) = 0$ then since $\mathbf{M}$ is a unimodular matrix and $m_{11}(\vartheta)m_{22}(\vartheta) - m_{12}(\vartheta)m_{21}(\vartheta) =$

1 it follows that

$$m_{11}(\vartheta)m_{22}(\vartheta) = 1 \text{ and } \eta = \frac{\lambda + \lambda^{-1}}{2}, \text{ where } \lambda = m_{11}(\vartheta) \text{ or } \lambda = m_{22}(\vartheta). \tag{32}$$

Using recurrent relation (27) the following relation can be shown for the Chebyshev polynomials of second kind:

$$\lambda S_n(\eta) - S_{n-1}(\eta) = \lambda((\lambda + \lambda^{-1})S_{n-1}(\eta) - S_{n-2}(\eta)) - S_{n-1}(\eta) = \lambda\left(\lambda S_{n-1}(\eta) - S_{n-2}(\eta)\right), \tag{33}$$

which can be written as

$$P_{n+1}(\eta) = \lambda P_n(\eta),$$

where $$P_n(\eta) = \lambda S_{n-1}(\eta) - S_{n-2}(\eta).$$

Taking into account that $P_1(\eta) = \lambda$, ($S_0(\eta) = 1, S_{-1}(\eta) = 0$) the following identity can be obtained valid for all integers starting from $n = 1$

$$P_n(\eta) = \lambda^n.$$

Hence it follows from (29) that for frequencies $\vartheta = \vartheta_0$, where ϑ_0 are the roots of $m_{12}(\vartheta) = 0$

$$u(nd) = \lambda^n u(0),\ n = 1, 2, ..., N. \tag{34}$$

2.1.1. The Case of Non-Uniform Distribution of Electrodes

It follows from (32) that $\lambda \neq 1$ if $m_{11}(\vartheta) \neq m_{22}(\vartheta)$, which takes place if $d_1 \neq d_2$. Therefore equation (34) shows that at frequencies $\vartheta = \vartheta_0$, where ϑ_0 are the roots of $m_{21}(\vartheta) = 0$, localisation of elastic shear displacements takes place at the top and bottom interfaces of the periodic waveguide if the electrodes are non-symmetrically placed through the waveguide.

2.1.2. The Case of Uniform Distribution of Electrodes

If $d_1 = d_2$ the transfer matrices are the same at consecutive interfaces ($\mathbf{T}_1 = \mathbf{T}_2$) and therefore $m_{11}(\vartheta) = m_{22}(\vartheta)$, which means $\lambda = \pm 1$. This means that symmetrically arranged electrodes do not support wave localization in the structure.

2.1.3. *Normal Modes of a Traction Free Waveguide*

Another possible case in equation (30) is $S_{N-1}(\eta) = 0$. This equation has $(N-1)$ roots in the interval $\eta \in (-1,1)$ which are given by $\eta_m = \cos\left(m\pi N^{-1}\right), m = 1,2,...(N-1)$. Taking into account that in this case $S_{N-2}(\eta_m) = (-1)^{m+1}$ [22] one can write

$$u(nd) = (-1)^m u(0),\ n = 1,2,...,N. \tag{35}$$

This means that $N-1$ shear wave normal modes exist where guided waves are distributed along the crystal width and have the same magnitude at the top and the bottom faces.

2.2. *Localisation and Normal Modes of a Clamped Waveguide*

When the the top and bottom faces of the periodic crystal are clamped $u(0) = u(L)$ equations (29) and (30) should be replaced by the following two equations:

$$m_{12}(\vartheta)S_{N-1}(\eta) = 0 \tag{36}$$

$$(m_{22}(\vartheta)S_{n-1}(\eta) - S_{n-2}(\eta))\sigma_0(0) = \sigma_0(nd), \tag{37}$$

$$\sigma(nd) = \lambda^n \sigma_0(0),\ n = 1,2,...N. \tag{38}$$

In this case the non-symmetric arrangement of electrodes leads to the localization of the elastic shear stresses at the top and bottom layers if $m_{12}(\vartheta) = 0$. There are also $N-1$ normal modes distributed along the crystal width and have the same magnitude of stresses at the top and the bottom faces which follows from the following relation:

$$\sigma_0(nd) = (-1)^m \sigma_0(0),\ n = 1,2,...,N.$$

Thus two different families of vibrational modes exist in the piezoelectric supperlattice for both fraction free and clamped top and bottom faces. One is a localized mode which exists only when the electrodes are non-symmetrically inserted through the thickness of the piezoelectric material ($d_1 \neq d_2$) and occurs at frequencies $m_{12}(\vartheta) = 0$ and $m_{21}(\vartheta) = 0$. There are also another $N-1$ normal non-localised vibration modes at frequencies defined by $S_{N-1}(\eta) = 0$ which exist in both cases when the electrodes are symmetrically ($d_1 = d_2$) or non-symmetrically inserted into the piezoelectric waveguide.

3. Discussion

Numerical calculations have been carried out for a piezoelectric superlattice made from PZT-4 with material parameters $c_{44} = 2.56 \cdot 10^{10} N/m^2$, $e_{15} = 12.7 C/m^2$, $\varepsilon_{11} = 646 \cdot 10^{-11} F/m$ and $\rho = 7.6 \cdot 10^3 kg/m^3$ [23].

For a superlattice of a finite width with non-symmetrically inserted electrodes through the thickness of the piezoelectric crystal ($d_1 \neq d_2$) for any value of dimensionless wave number kd and $\delta = d_1/d \neq 0.5$ there always are infinite number of discrete spectrum of eigenfrequencies which correspond to localised vibrations. These eigenfrequencies shown in Figures 2(a,b) are the solutions of dispersion equations $m_{12}(\vartheta) = 0$ and $m_{21}(\vartheta) = 0$ and at these frequencies $m_{11}(\vartheta) \neq \pm 1$.

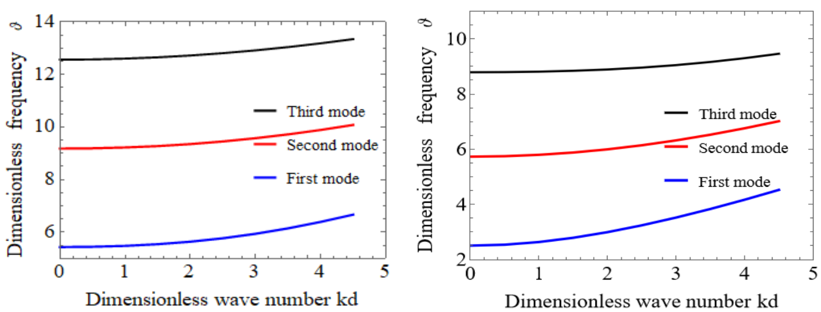

(a) (b)

Figure 2: First three modes of dispersion curves of equation a) $m_{12}(\vartheta) = 0$ (clamped top and bottom faces) and b) $m_{21}(\vartheta) = 0$ (traction free top and bottom faces) for $\delta = 0.25$ (the same for $\delta = 0.75$).

The localization coefficient $|\lambda|$ for both cases depending on the relative thickness δ are shown in Figures 3, 4 at different points of the dispersion curves. At equidistant from the top and bottom interfaces of the supperlattice $\vartheta^*(kd, \delta) = \vartheta^*(kd, 1-\delta) = \vartheta^*$ and $\lambda(\vartheta^*, \delta) = \lambda(\vartheta^*, 1-\delta) = 1$ for any root ϑ^* of the equations $m_{12}(\vartheta) = 0$ or $m_{21}(\vartheta) = 0$.

Figure 3, where $\lambda = |m_{22}(\vartheta)|$, corresponds to the localization of shear stresses for the supperlattice with clamped top and bottom faces. Figure 4, where $\lambda = |m_{11}(\vartheta)|$, corresponds to the localization of elastic displacements for the supperlattice with traction free top and bottom faces. It follows from (34) and (38) that in the case of $\lambda < 1$ the localization of guided waves takes place at the top face of the waveguide and in the

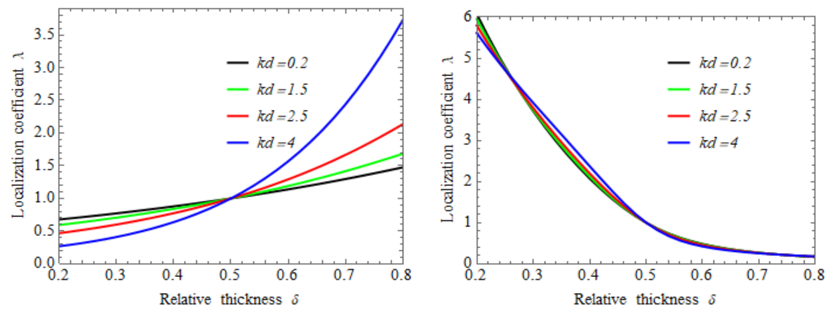

(a) (b)

Figure 3: Localization coefficients for electro-elastic shear stresses, $\lambda = |m_{22}(\vartheta)|$, for the supperlattice with traction free top and bottom faces a) the first frequency mode and b) the second frequency mode.

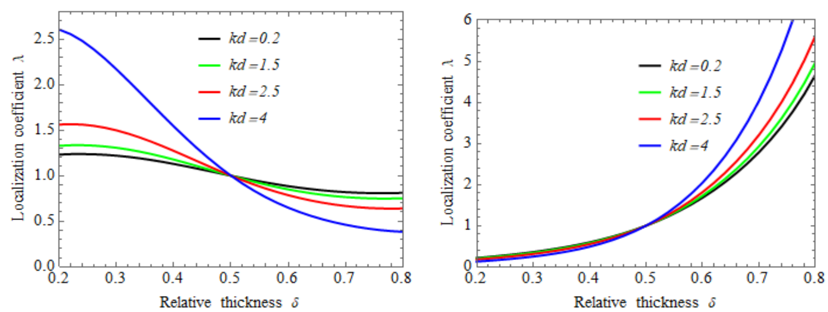

(a) (b)

Figure 4: Localization coefficients for elastic displacements, $\lambda = |m_{11}(\vartheta)|$, for the supperlattice with clamped top and bottom faces a) the first frequency mode and b) the second frequency mode.

case of $\lambda > 1$ the waves localise at the bottom face. In the piezoelectric waveguide the closest electrode from the bottom face is at the distance d_1 from it and the closest electrode from the top face is at the distance d_2 from it. For a waveguide with traction free top and bottom faces the amplitudes of shear displacements for the first mode attenuate from the top layers to the bottom layers if $d_1/d_2 < 1$ and from the bottom layers to the top layers if $d_1/d_2 > 1$ (Fig. 3(a)). For the second mode the waves localise at the top layer for $d_1/d_2 > 1$ and at the bottom layer if $d_1/d_2 < 1$ (Fig 3(b)).

On the contrary for a waveguide with clamped interfaces for the first mode the amplitude of shear stresses attenuate from the bottom to the top layers if $d_1/d_2 < 1$ and from the top to the bottom layers if $d_1/d_2 > 1$ (Fig. 4(a)) and for the second mode waves localise at the top of the waveguide if $d_1/d_2 < 1$ and at the bottom of the waveguide if $d_1/d_2 > 1$ (Fig. 4(b)) . For a finite waveguide the amplitude of a guided wave for $N \geq 10$ becomes negligibly small at depths of more than a few wavelengths. The disturbance is therefore strongly confined to layers close to the top or bottom faces of the waveguide.

Dispersion curves in Fig. 2 define the dependence of normalized frequency on the dimensionless wave number kd. For fixed values of d the dimensional vibration eigenfrequency can be calculated using the formula

$$\omega(d) = \vartheta\sqrt{\frac{G+e^2/\varepsilon}{d^2\rho}}. \tag{39}$$

As it follows from Fig. 3 and Fig. 4 a strong localization of guided waves takes place at $kd = 4$ for first modes at $\vartheta \approx 6.5$ for a clamped waveguide and $\vartheta \approx 4.1$ for a traction free waveguide. For $d = d_1 + d_2 = 2 * 10^{-2}$m these correspond to dimensional frequencies $\omega \approx 0.84$ MHz and $\omega \approx 0.53$ MHz. Typical dimensions between electrodes in such structures is between $d = 10^{-3}$m and $d = 10^{-2}$m. For example in experiments carried out in [24] for a piezoelectric material inserted with thin electrodes the distance between electrodes is taken 10^{-2}m.

There is a very strong localization of the guided wave amplitudes depending on the arrangements of the electrodes through the thickness of the piezoelectric waveguide. The guided wave localization changes also with the vibration frequency modes and the dimensionless wave numbers although this dependence is weaker for the second frequency modes.

In an infinite periodic structure for any values of dimensionless wave number kd the condition $|\eta| > 1$ defines intervals of frequencies called forbidden frequencies where waves cannot propagate [25]. In the case of infinite periodic structure the problem of the interfacial effects of the periodic piezoelectric structure was considered in [5] where it was shown that in the piezoelectric structure with inserted electrodes the forbidden frequency intervals of electro-elastic waves defined by the equation $|\eta(\vartheta^*) > 1$ have a very weak dependence on the filling coefficient δ. For the finite structure under consideration the localization effect strongly depends on the filling coefficient δ

at frequencies ϑ^* where $|\eta(\vartheta^*) > 1$ and stop occurring for symmetrically inserted electrodes ($\delta = 0.5$).

4. Conclusion

Localization of electro-elastic shear waves takes place in a finite periodically stratified homogeneous piezoelectric structure with periodically inserted electrodes of negligible width. Two different families of vibrational modes propagate through the piezoelectric supperlattice for both traction free and clamped top and bottom faces. One of them is a localized mode which occurs only when the electrodes are non-uniformly distributed through the thickness of the piezoelectric material. The localisation can be either of the amplitudes of electro-elestic stresses or elastic displacements depending on the boundary conditions on the top and bottom faces of the structure. The transfer matrix between two neighbouring sub-layers is constructed with electrically shorted interfacial conditions. It is shown that due to the electro-mechanical coupling waves can be strongly localized at interfaces of the structure if the electrods are non-symmetrically distributed along the thickness of the piezoelectric material. The localization of waves significantly increases with the numbers of non-symmetrically introduced electrodes between the layers and disappears if the electrodes are evenly distributed.

Controlling wave propagation properties in finite piezoelectric periodic structures can be helpful in the design of narrow band filters or multi-channel piezoelectric filters. The results of this paper can also have applications in designing tunable waveguides made of layers of identical piezoelectric crystals.

It is worth mentioning, that conventional manufacturing methods for embedding metals into piezoelectric materials can be difficult due to their high processing temperatures and long curing times of the adhesives applied for bonding the piezoelectric component to the metal. Manufacturing processes of a fabrication procedure for embedding electrodes into piezoelectric body is presented in [26]. The proposed fabrication process could be effectively realised for rapid fabrication of functionalized metal structures which can be used in thermal measurements, energy harvesting, and structural health monitoring applications. Experimental results for artificially fabricated piezoelectric plates and rods with electrodes have also been reported in [27] and [28] .

5. Acknowledgments

This work was supported by the RA MES Science Committee in the framework of the research project № 21T-2C299.

References

[1] A. K. Vashishth, V. Gupta, Wave propagation in transversely isotropic porous piezoelectric materials, International Journal of Solids and Structures 46 (20) (2009) 3620–3632. doi:https://doi.org/10.1016/j.ijsolstr.2009.06.011.

[2] Y. Wang, F. Li, K. Kishimoto, Y. Wang, W. Huang, Elastic wave band gaps in magnetoelectroelastic phononic crystals, Wave Motion 46 (1) (2009) 47–56. doi:http://doi.org/10.1016/j.wavemoti.2008.08.001.

[3] M. Wilm, S. Ballandras, V. Laude, T. Pastureaud, A full 3d plane-wave-expansion model for 1-3 piezoelectric composite structures, The Journal of the Acoustical Society of America 112 (3) (2002) 943–952. doi:10.1121/1.1496081. PMID: 12243182.

[4] X. Zou, Q. Chen, B. Liang, J. Cheng, Control of the elastic wave bandgaps in two-dimensional piezoelectric periodic structures, Smart Materials and Structures 17 (1) (2008) 015008(1–8). doi:10.1088/0964-1726/17/01/015008.

[5] K. Ghazaryan, D. Piliposyan, Interfacial effects for shear waves in one dimensional periodic piezoelectric structure, Journal of Sound and Vibration 330 (26) (2011) 6456 – 6466. doi:https://doi.org/10.1016/j.jsv.2011.08.011.

[6] G. Piliposian, A. Avetisyan, K. Ghazaryan, Shear wave propagation in periodic phononic/photonic piezoelectric medium, Wave Motion 49 (1) (2012) 125–134. doi:https://doi.org/10.1016/j.wavemoti.2011.08.001.

[7] F. Sabina, A. Movchan, Interfacial effects in electromagnetic coupling within piezoelectric phononic crystals, Acta Mechanica Sinica 25 (1) (2009) 95–99. doi:http://DOI 10.1007/s10409-008-0201-y.

[8] V. Alshits, A. Gorkunova, A. Shuvalov, Phase resonance in the reflection of acoustic waves by a system of piezocrystalline layers separated by cladding layers with screening properties, Journal Of Experimental and Theoretical Physics 83 (1996) 509–516.

[9] A. Shuvalov, A. Gorkunova, Transverse acoustic waves in piezoelectric and ferroelectric antiphase superlattices, Physical Review B 59 (14) (1999) 9070–9077.

[10] Y. Guo, W. Chen, Y. Zhang, Guided wave propagation in multilayered piezoelectric structures, Science in China: Physics, Mechanics and Astronomy 52 (7) (2009) 1094–1104. doi:https://doi.org/10.1007/s11433-009-0130-1.

[11] P. Shi, C. Chen, W. Zou, Propagation of shear elastic and electromagnetic waves in one dimensional piezoelectric and piezomagnetic composites, Ultrasonics 55 (2015) 42—47. doi:https://doi.org/10.1016/j.ultras.2014.08.011.

[12] D. Piliposyan, G. Piliposian, K. Ghazaryan, Propagation and control of shear waves in piezoelectric composite waveguides with metallized interfaces, International Journal of Solids and Structures 106–107 (2017) 119 – 128. doi:https://doi.org/10.1016/j.ijsolstr.2016.11.027.

[13] R. L. Thomes, J. A. Mosquera-Sánchez, C. D. Marqui, Bandgap widening by optimized disorder in one-dimensional locally resonant piezoelectric metamaterials, Journal of Sound and Vibration 512 (2021) 116369. doi:https://doi.org/10.1016/j.jsv.2021.116369.

[14] Y. Liu, D. Yu, L. Li, H. Zhao, J. Wen, X. Wen, Design guidelines for flexural wave attenuation of slender beams with local resonators, Physics Letters A 362 (5) (2007) 344–347. doi:https://doi.org/10.1016/j.physleta.2006.10.056.

[15] A. Chen, F. Li, Y.-S. Wang, Localization of flexural waves in a disordered periodic piezoelectric beam, Journal of Sound and Vibration 304 (2007) 863–874. doi:10.1016/j.jsv.2007.03.047.

[16] Z.-Z. Yan, C. Zhang, Y.-S. Wang, Attenuation and localization of bending waves in a periodic/disordered fourfold composite beam, Journal of Sound and Vibration 327 (1) (2009) 109–120. doi:https://doi.org/10.1016/j.jsv.2009.06.009.

[17] A. Baxy, R. Prasad, A. Banerjee, Elastic waves in layered periodic curved beams, Journal of Sound Vibration 512 (2021) 116387. doi:10.1016/j.jsv.2021.116387.

[18] K. Nakamura, Elastic wave energy-trapping and its application to piezoelectric devices, Electronics and Communications in Japan (Part II: Electronics) 79 (7) (1996) 30–39.

[19] F. Kobayashi, S. Biwa, N. Ohno, Wave transmission characteristics in periodic media of finite length: multilayers and fiber arrays, International Journal of Solids and Structures 41 (26) (2004) 7361–7375.

[20] Y. Xu, Spatial bandwidth enlargement and field enhancement of shear horizontal waves in finite graded piezoelectric layered media, Physics Letters A 379 (30) (2015) 1752–1756. doi:https://doi.org/10.1016/j.physleta.2015.04.005.

[21] D. Piliposyan, K. Ghazaryan, G. Piliposian, Shear bloch waves and coupled phonon–polariton in periodic piezoelectric waveguides, Ultrasonics 54 (2) (2014) 644–654. doi:https://doi.org/10.1016/j.ultras.2013.09.018.

[22] A. A. Tovar, L. W. Casperson, Generalized sylvester theorems for periodic applications in matrix optics, J. Opt. Soc. Am. A 12 (3) (1995) 578–590.

[23] B. Collet, M. Destrade, G. A. Maugin, Bleustein–gulyaev waves in some functionally graded materials, European Journal of Mechanics - A/Solids 25 (5) (2006) 695–706. doi:https://doi.org/10.1016/j.euromechsol.2006.01.007.

[24] S. Degraeve, C. Granger, B. Dubus, J. O. Vasseur, M. Pham Thi, A. C. Hladky-Hennion, Bragg band gaps tunability in an homogeneous piezoelectric rod with periodic electrical boundary conditions., Journal of applied Physics 115 (19) (2015) 194508. doi:10.1088/0964-1726/24/8/085013.

[25] A. Srivastava, Metamaterial properties of periodic laminates, Journal of the Mechanics and Physics of Solids 96 (2016) 252–263. doi:https://doi.org/10.1016/j.jmps.2016.07.018.

[26] A. K. Ramanathan, M. B. Gingerich, L. M. Headings, M. J. Dapino, Metal structures embedded with piezoelectric pvdf sensors using ultrasonic additive manufacturing, Manufacturing Letters 31 (2022) 96–100. doi:https://doi.org/10.1016/j.mfglet.2021.08.001.

[27] S. Degraeve, C. Granger, B. Dubus, J. O. Vasseur, M. P. Thi, A.-C. Hladky, Tunability of bragg band gaps in one-dimensional piezoelectric phononic crystals using external capacitances, Smart Materials and Structures 24 (8) (2015) 085013. doi:10.1088/0964-1726/24/8/085013.

[28] C. Croenne, M. fraise Ponge, B. Dubus, C. Granger, L. Haumesser, F. Levassort, J. Vasseur, A. Lordereau, M. P. Thi, A.-C. Hladky-Hennion, Tunable phononic crystals based on piezoelectric composites with 1-3 connectivity., The Journal of the Acoustical Society of America 139 6 (2016) 3296.